

1 **Soil moisture control on sap flow response to biophysical factors in a desert-shrub**
2 **species, *Artemisia ordosica***

3 **Authors:** Tianshan Zha^{1,3*#}, Duo Qian^{2#}, Xin Jia^{1,3}, Yujie Bai¹, Yun Tian¹, Charles P.-A.
4 Bourque⁴, Wei Feng¹, Bin Wu¹, Heli Peltola⁵

5 ¹. Yanchi Research Station, School of Soil and Water Conservation, Beijing Forestry
6 University, Beijing 100083, China

7 ². Beijing Vocational College of Agriculture, Beijing 102442, China

8 ³. Key Laboratory of State Forestry Administration on Soil and Water Conservation, Beijing
9 Forestry University, Beijing, China

10 ⁴. Faculty of Forestry and Environmental Management, 28 Dineen Drive, PO Box 4400,
11 University of New Brunswick, New Brunswick, E3B5A3, Canada

12 ⁵. Faculty of Science and Forestry, School of Forest Sciences, University of Eastern Finland,
13 Joensuu, FI-80101, Finland

14 #These authors contributed equally to this work.

15

16

17 **Short title: Sap flow in *Artemisia ordosica***

18

19

20 *Correspondence to:* T. Zha (tianshanzha@bjfu.edu.cn),

21

22 **Author Contribution Statement:**

23 Dr.'s Duo Qian and Tianshan Zha contributed equally to the design and implementation of
24 the field experiment, data collection and analysis, and writing the first draft of the manuscript.

25 Dr. Xin Jia gave helpful suggestions concerning the analysis of the field data and contributed
26 to the scientific revision and editing of the manuscript.

27 Prof. Bin Wu contributed to the design of the experiment.

28 Dr.'s Charles P.-A. Bourque and Heli Peltola contributed to the scientific revision and editing
29 of the manuscript.

30 Yujie Bai, Wei Feng, and Yun Tian were involved in the implementation of the experiment
31 and in the revision of the manuscript.

32

33 **Key Message:** This study provides a significant contribution to the understanding of
34 acclimation processes in desert-shrub species to drought-associated stress in dryland
35 ecosystems

36

37 **Conflict of Interest:**

38 This research was financially supported by grants from the National Natural Science
39 Foundation of China (NSFC No. 31670710, No. 31670708), the National Basic Research
40 Program of China (Grant No. 2013CB429901), and by the Academy of Finland (Project No.
41 14921). The project is related to the Finnish-Chinese collaborative research project,
42 EXTREME (2013-2016), between Beijing Forestry University and the University of Eastern
43 Finland, and USCCC. We appreciate Dr. Ben Wang, Sijing Li, Qiang Yang, and others for
44 their help with the fieldwork. The authors declare that they have no conflict of interest.

45

46 **Abstract:** Current understanding of acclimation processes in desert-shrub species to drought
47 stress in dryland ecosystems is still incomplete. In this study, we measured sap flow in
48 *Artemisia ordosica* and associated environmental variables throughout the growing seasons
49 of 2013 and 2014 (May-September period of each year) to better understand the
50 environmental controls on the temporal dynamics of sap flow. We found that the occurrence
51 of drought in the dry year of 2013 during the leaf-expansion and leaf-expanded periods
52 caused sap flow per leaf area (J_s) to decline significantly, resulting in transpiration being 34%
53 lower in 2013 than in 2014. J_s correlated positively with radiation (R_s), air temperature (T),
54 and water vapor pressure deficit (VPD), when volumetric soil water content (VWC) was >
55 $0.10 \text{ m}^3 \text{ m}^{-3}$. There was a time lag of as much as six hours between diurnal J_s and R_s . This
56 hysteresis effect, however, decreased with increasing VWC. Relative response of J_s to the
57 environmental variables (i.e., R_s , T , and VPD) varied with VWC, J_s being more strongly
58 controlled by plant-physiological processes during periods of dryness indicated by a low
59 decoupling coefficient and low sensitivity to the environmental variables. According to this
60 study, soil moisture is shown to control J_s (and, therefore, plant-transpiration) response in
61 *Artemisia ordosica* to diurnal variations in biophysical factors. This species acclimated to
62 water limitations by invoking a water-conservation strategy with the regulation of stomatal
63 conductance and advancement of J_s peaking time, manifesting in a hysteresis effect. The
64 findings of this study add to the knowledge of acclimation processes in desert-shrub species
65 under drought-associated stress.

66 **Keywords:** sap flow; transpiration; cold-desert shrubs; environmental stress; volumetric soil
67 water content

68

69

70 **1. Introduction**

71 Due to the low amount of precipitation and high potential evapotranspiration in desert
72 ecosystems, low soil water availability limits both plant water- and gas-exchange and, as a
73 consequence, limits vegetation productivity (Razzaghi et al., 2011). Shrub and semi-shrub
74 species are replacing grass species in arid and semi-arid lands in response to ongoing
75 aridification of the land surface (Huang et al., 2011a). This progression is predicted to
76 continue under a changing climate (Houghton et al., 1999; Pacala et al., 2001; Asner et al.,
77 2003). Studies have shown that desert shrubs are able to adapt to hot-dry environments as a
78 result of their small plant-surface area, thick epidermal hairs, and large root-to-shoot ratios
79 (Eberbach and Burrows, 2006; Forner et al., 2014). Plant traits related to water use are likely
80 to adapt differentially with species and habitat type (Brouillette et al., 2014). Plants may
81 select water-acquisition or water-conservation strategies in response to water limitations
82 (Brouillette et al., 2014). Knowledge of physiological acclimation of changing species to
83 water shortages in deserts, particularly with respect to transpiration, is inadequate and, in the
84 context of plant adaptation to changing climatic conditions, is of immense interest (Jacobsen
85 et al., 2007; Huang et al., 2011a). Transpiration is controlled by stomatal through changing
86 its conductance and pores, and its magnitude and timing is related to the prevailing
87 biophysical factors (Jarvis 1976; Jarvis and McNaughton, 1986).

88 Sap flow can be used to reflect species-specific water consumption by plants (Ewers et
89 al., 2002; Baldocchi, 2005; Naithani et al., 2012). Sap flow can also be used to continuously
90 monitor canopy conductance and its response to environmental variables (Ewers et al., 2007;
91 Naithani et al., 2012). Stomatal conductance at the plant scale exerts a large biotic control on
92 transpiration particularly during dry conditions (Jarvis 1976; Jarvis and McNaughton, 1986).
93 Stomatal conductance couples photosynthesis and transpiration (Cowan and Farquhar, 1977),
94 making this parameter an important component of climate models in quantifying biospheric-
95 atmospheric interactions (Baldocchi et al., 2002).

96 Studies have shown that xylem hydraulic conductivity was closely correlated with
97 drought resistance (Cochard et al., 2008, 2010; Ennajeh et al., 2008). With increasing aridity,
98 trees can progressively lessen their stomatal conductance, resulting in lower transpiration
99 (McAdam et al., 2016). Generally, desert shrubs can close their stomata, reducing stomatal
100 conductance, and reduce their water consumption when exposed to dehydration stresses.
101 However, differences exist among shrub species in terms of their stomatal response to
102 changes in air and soil moisture deficits (Pacala et al., 2001).

103 In *Elaeagnus angustifolia*, transpiration is observed to peak at noon, i.e., just before
104 stomatal closure under water-deficit conditions (Liu et al., 2011), peaking earlier than
105 radiation, temperature, and water vapor pressure deficit. This response lag or hysteresis effect
106 has been widely noticed in dryland species (Du et al., 2011; Naithani et al., 2012), but its

107 function is not completely understood. Transpiration in *Hedysarum scoparium* peaks
108 multiple times during the day. For other shrubs, sap flow has been observed to decrease
109 rapidly when the volumetric soil water content is lower than the water lost through
110 evapotranspiration (Buzkova et al., 2015). Sap flow in *Caragana korshinskii* and *Hippophae*
111 *rhamnoides* has been found to increase with increasing rainfall intensity (Jian et al., 2016),
112 whereas in *Haloxylon ammodendron*, it was found to vary in response to rainfall, from an
113 immediate decline after a heavy rainfall to no observable change after a small rainfall event
114 (Zheng and Wang, 2014). Drought-insensitive shrubs have relatively strong stomatal
115 regulation and, therefore, tend to be insensitive to soil water deficits and rainfall, unlike their
116 drought-sensitive counterparts (Du et al., 2011). Support for the relationship between sap
117 flow in desert shrubs and prevailing environmental factors is decidedly variable (McDowell
118 et al., 2013; Sus et al., 2014), potentially varying with plant habitat and species (Liu et al.,
119 2011).

120 *Artemisia ordosica*, a shallow-rooted desert shrub, is the dominant species in the Mu Us
121 Desert of northwestern China. It plays an important role in combating desertification and in
122 stabilizing sand dunes (Li et al., 2010). Increases in air temperature and precipitation
123 variability and associated shorter wet and longer dry periods are expected to ensue under
124 changing climate change (Lioubimtseva and Henebry, 2009). Sap flow in *Artemisia ordosica*
125 has been observed to be controlled by soil water content at about a 30-cm depth in the soil
126 during dry periods of the year (Li et al., 2014). However, our understanding of the
127 mechanisms of desert-shrub acclimation during periods of water shortage remains
128 incomplete. Questions needing answering from our research include (1) how do changes in
129 sap flow relate to changes in biotic and abiotic factors, and (2) whether *Artemisia ordosica*
130 selects a strategy of water-conservation or water-acquisition under conditions of drought? To
131 attend to these questions, we continuously measured stem sap flow in *Artemisia ordosica* and
132 associated environmental variables *in situ* throughout the growing seasons of 2013 and 2014
133 (May-September period of each year). Our findings present insights concerning the main
134 environmental factors affecting transpiration in *Artemisia ordosica*, e.g., optimal temperature,
135 water vapor pressure deficit, and soil water content. This understanding can lead to improving
136 phytoremediation practices in desert-shrub ecosystems.

137

138 **2. Materials and Methods**

139 **2.1 Experimental site**

140 Continuous sap flow measurements were made at the Yanchi Research Station (37°42' 31"
141 N, 107°13' 47" E, 1530 m above mean sea level), Ningxia, northwestern China. The
142 research station is located between the arid and semi-arid climatic zones along the southern
143 edge of the Mu Us Desert. The sandy soil in the upper 10 cm of the soil profile has a bulk

144 density of $1.54 \pm 0.08 \text{ g cm}^{-3}$ (mean \pm standard deviation, $n=16$). Mean annual precipitation
145 in the region is about 287 mm, of which 62% falls between July and September. Mean annual
146 potential evapotranspiration and air temperature are about 2,024 mm and 8.1°C based on
147 meteorological data (1954-2004) from the Yanchi County weather station. Normally, shrub
148 leaf-expansion, leaf-expanded, and leaf-coloration stages begin in April, June, and
149 September, respectively (Chen et al., 2015).

150

151 **2.2 Environmental measurements**

152 Shortwave radiation (R_s in W m^{-2} ; CMP3, Kipp & Zonen, Netherland), air temperature (T in
153 $^\circ\text{C}$), wind speed (u in m s^{-1} , 034B, Met One Instruments Inc., USA), and relative humidity
154 (RH in %; HMP155A, Väisälä, Finland) were measured simultaneously near the sap flow
155 measurement plot. Half-hourly data were recorded by data logger (CR3000 data logger,
156 Campbell Scientific Inc., USA). Volumetric soil water content (VWC) at a 30-cm depth were
157 measured using three ECH₂O-5TE soil moisture probes (Decagon Devices, USA). In the
158 analysis, we used half-hourly averages of VWC from the three soil moisture probes. Water
159 vapor pressure deficit (VPD in kPa) was calculated from recorded RH and T .

160

161 **2.3 Measurements of sap flow, leaf area and stomatal conductance**

162 The experimental plot ($10 \text{ m} \times 10 \text{ m}$) was located on the western side of Yanchi Research
163 Station in an *Artemisia ordosica*-dominated area. Mean age of the *Artemisia ordosica* was
164 10-years old. Maximum monthly mean leaf area index (LAI) for plant specimens with full
165 leaf expansion was about $0.1 \text{ m}^2 \text{ m}^{-2}$ (Table 1). Over 60% of their roots were distributed in the
166 first 60 cm of the soil complex (Zhao et al., 2010; Jia et al., 2016). Five stems of *Artemisia*
167 *ordosica* were randomly selected within the plot as replicates for sap flow measurement.
168 Mean height and sapwood area of sampled shrubs were 84 cm and 0.17 cm^2 , respectively.
169 Sampled stems represented the average size of stems in the plot. A heat-balance sensor
170 (Flow32-1K, Dynamax Inc., Houston, USA) was installed at about 15 cm above the ground
171 surface on each of the five stems (Dynamax, 2005). Sap flow measurements from each stem
172 were taken once per minute. Half-hourly data were recorded by a Campbell CR1000 data
173 logger from May 1 to September 30, for both 2013 and 2014 (Campbell Scientific, Logan,
174 UT, USA).

175 Leaf area was estimated for each stem every 7-10 days by sampling about 50-70 leaves
176 from five randomly sampled neighboring shrubs with similar characteristics to the shrubs
177 being used for sap flow measurements. Leaf area was measured immediately at the station
178 laboratory with a portable leaf area meter (LI-3000, Li-Cor, Lincoln, NE, USA). Leaf area
179 index (LAI) was measured on a weekly basis from a 4×4 grid of 16 quadrats ($10 \text{ m} \times 10 \text{ m}$
180 each) within a $100 \text{ m} \times 100 \text{ m}$ plot centered on a flux tower using measurements of sampled

181 leaves and allometric equations (Jia et al., 2014). Stomatal conductance (g_s) was measured *in*
 182 *situ* for three to four leaves on each of the sampled shrubs with a LI-6400 portable
 183 photosynthesis analyzer (Li-Cor Inc., Lincoln, USA). The g_s measurements were made every
 184 two hours from 7:00 to 19:00 h every ten days from May to September, 2013 and 2014.

185 Biotic and abiotic effects on sap flow and transpiration are often interactive and
 186 confounded. The decoupling coefficient (Ω) was used to examine the relative contribution of
 187 biotic control through stomatal regulation of transpiration (Jarvis and McNaughton, 1986).
 188 Stomatal regulation becomes stronger as Ω approaches zero. The decoupling coefficient
 189 varies from zero (i.e., leaf transpiration is mostly controlled by g_s) to one (i.e., leaf
 190 transpiration is mostly controlled by radiation). The Ω was calculated as described by Jarvis
 191 and McNaughton (1986), i.e.,

$$192 \quad \Omega = \frac{\Delta + \gamma}{\Delta + \gamma \left(1 + \frac{g_a}{g_s} \right)}, \quad (1)$$

193 where Δ is the rate of change of saturation vapor pressure vs. temperature (kPa K^{-1}), γ is the
 194 psychrometric constant (kPa K^{-1}), and g_a is the aerodynamic conductance (m s^{-1} ; Monteith
 195 and Unsworth, 1990),

$$196 \quad g_a = \left(\frac{u}{u^{*2}} + 6.2u^{*-0.67} \right)^{-1}, \quad (2)$$

197 where u is the wind speed (m s^{-1}) at 6 m above the ground, and u^* is the friction velocity (m
 198 s^{-1}), measured by a nearby eddy covariance system (Jia et al., 2014).

199

200 **2.4 Data analysis**

201 In our analysis, drought days were defined as those days with daily mean VWC $< 0.1 \text{ m}^3 \text{ m}^{-3}$.
 202 This is based on a VWC threshold of $0.1 \text{ m}^3 \text{ m}^{-3}$ for J_s (Fig. 1), with J_s increasing as VWC
 203 increased, saturating at VWC of $0.1 \text{ m}^3 \text{ m}^{-3}$, and decreasing as VWC continued to increase.
 204 The VWC threshold of $0.1 \text{ m}^3 \text{ m}^{-3}$ is equivalent to a relative extractable soil water (REW) of
 205 0.4 for drought conditions (Granier et al., 1999 and 2007; Zeppel et al., 2004 and 2013; Fig.
 206 2d, e). Duration and severity of ‘drought’ were defined based on a VWC threshold and REW
 207 of 0.4. REW was calculated with

$$208 \quad REW = \frac{VWC - VWC_{\min}}{VWC_{\max} - VWC_{\min}}, \quad (3)$$

209 where VWC is the specific daily soil water content ($\text{m}^3 \text{ m}^{-3}$), VWC_{\min} and VWC_{\max} are the
 210 minimum and maximum VWC during the measurement period in each year, respectively.

211 Sap flow analysis was conducted using mean data from five sensors. Sap flow per leaf
 212 area (J_s , $\text{kg m}^{-2} \text{ h}^{-1}$ or $\text{kg m}^{-2} \text{ d}^{-1}$) was calculated according to

$$J_s = \left(\sum_{i=1}^n E_i / A_{li} \right) / n, \quad (4)$$

where E is the measured sap flow of a stem (g h^{-1}), A_l is the leaf area of the sap flow stem, and “ n ” is the number of stems sampled ($n = 5$).

Transpiration per ground area (T_r) was estimated in this study according to:

$$T_r = \left(\sum_{i=1}^n J_s \times LAI \right) / n, \quad (5)$$

where T_r is transpiration per ground area (mm d^{-1}).

Linear and non-linear regressions were used to analyze abiotic control on sap flow. In order to minimize the effects of different phenophases and rainfall, we only used data from the mid-growing season, non-rainy days, and daytime hours from 8:00-20:00, i.e., from June 1 to August 31, with hourly shortwave radiation $> 10 \text{ W m}^{-2}$. Relations between mean sap flow at specific times over a period of 8:00-20:00 and corresponding environmental factors from June 1 to August 31 were derived from linear regression ($p < 0.05$; Fig. 3). Regression slopes were used as indicators of sap flow sensitivity (degree of response) to the various environmental variables (see e.g., Zha et al., 2013). All statistical analyses were performed with SPSS v. 17.0 for Windows software (SPSS Inc., USA). Significance level was set at 0.05.

3. Results

3.1 Seasonal variations in environmental factors and sap flow

The range of daily means (24-hour mean) for R_s , T , VPD, and VWC during the 2013 growing season (May-September) were $31.1\text{-}364.9 \text{ W m}^{-2}$, $8.8\text{-}24.4^\circ\text{C}$, $0.05\text{-}2.3 \text{ kPa}$, and $0.06\text{-}0.17 \text{ m}^3 \text{ m}^{-3}$ (Fig. 2a, b, c, d), respectively, annual means being 224.8 W m^{-2} , 17.7°C , 1.03 kPa , and $0.08 \text{ m}^3 \text{ m}^{-3}$. Corresponding range of daily means for 2014 were $31.0\text{-}369.9 \text{ W m}^{-2}$, $7.1\text{-}25.8^\circ\text{C}$, $0.08\text{-}2.5 \text{ kPa}$, and $0.06\text{-}0.16 \text{ m}^3 \text{ m}^{-3}$ (Fig. 2a, b, c, d), respectively, annual means being 234.9 W m^{-2} , 17.2°C , 1.05 kPa , and $0.09 \text{ m}^3 \text{ m}^{-3}$.

Total precipitation and number of days with rainfall events during the 2013 measurement period (257.2 mm and 46 days) were about 5.6% and 9.8% lower than those during 2014 (272.4 mm and 51 days; Fig. 2d), respectively. More irregular rainfall events occurred in 2013 than in 2014, with 45.2% of rainfall falling in July and 8.8% in August.

Drought mainly occurred in May, June, and August of 2013 and in May and June of 2014 (shaded sections in Fig. 2d, e). Both years had dry springs. Over a one-month period of summer drought occurred in 2013.

The range of daily J_s during the growing season was $0.01\text{-}4.36 \text{ kg m}^{-2} \text{ d}^{-1}$ in 2013 and $0.01\text{-}2.91 \text{ kg m}^{-2} \text{ d}^{-1}$ in 2014 (Fig. 2f), with annual means of $0.89 \text{ kg m}^{-2} \text{ d}^{-1}$ in 2013 and 1.31

247 kg m⁻² d⁻¹ in 2014. Mean daily J_s over the growing season of 2013 was 32% lower than that
248 of 2014. Mean daily T_r were 0.05 mm d⁻¹ and 0.07 mm d⁻¹ over the growing season of 2013
249 and 2014 (Fig. 2f), respectively, being 34% lower in 2013 than in 2014. The total T_r over the
250 growing season (May 1-September 30) of 2013 and 2014 were 7.3 mm and 10.9 mm,
251 respectively. Seasonal fluctuations in J_s and T_r corresponded with seasonal patterns in VWC
252 (Fig. 2d, f). Daily mean J_s and T_r decreased or remained nearly constant during dry-soil
253 periods (Fig. 2d, f), with the lowest J_s and T_r observed in spring and mid-summer (August)
254 of 2013.

255

256 **3.2 Sap flow response to environmental factors**

257 In summer, J_s increased with increasing VWC, R_s , T , and VPD (Fig. 2d, f; Fig. 3). Sap flow
258 increased more rapidly with increases in R_s , T , and VPD under high VWC (i.e., VWC > 0.1
259 m³ m⁻³ in both 2013 and 2014; Fig. 4) compared with periods with lower VWC (i.e., VWC
260 < 0.1 m³ m⁻³ in both 2013 and 2014; Fig. 4). J_s was more sensitive to R_s , T , and VPD under
261 high VWC (Fig. 4), which coincided with a steeper regression slope under high VWC
262 conditions.

263 Sensitivity of J_s to environmental variables (in particular, R_s , T , VPD, and VWC) varied
264 depending on time of day (Fig. 5). Regression slopes for the relations of J_s - R_s , J_s - T , and J_s -
265 VPD were greater in the morning before 11:00 h, and lower during mid-day and early
266 afternoon (12:00-16:00 h). In contrast, regression slopes of the relation of J_s -VWC were
267 lower in the morning (Fig. 5), increasing thereafter, peaking at ~13:00 h, and subsequently
268 decreasing in late afternoon. Regression slopes of the response of J_s to R_s , T , and VPD in
269 2014 were steeper than those in 2013.

270

271 **3.3 Diurnal changes and hysteresis between sap flow and environmental factors**

272 Diurnal patterns of J_s were similar in both years (Fig. 6), initiating at 7:00 h and increasing
273 thereafter, peaking before noon (12:00 h), and subsequently decreasing thereafter and
274 remaining near zero from 20:00 to 6:00 h. Diurnal changes in g_s were similar to J_s , but
275 peaking about 2 and 1 h earlier than J_s in July and August, respectively (Fig. 6).

276 There were pronounced time lags between J_s and R_s over the two years (Fig. 7), J_s
277 peaking earlier than R_s and, thus, earlier than either VPD or T . These time lags differed
278 seasonally. For example, mean time lag between J_s and R_s was 2 h during July, 5 h during
279 May, and 3 h during June, August, and September of 2013. However, the time lags in 2014
280 were generally shorter than those observed in 2013 (Table 2).

281 Clockwise hysteresis loops between J_s and R_s during the growing period were observed
282 (Fig. 7). As R_s increased in the morning, J_s increased until it peaked at ~10:00 h. J_s declined
283 with decreasing R_s during the afternoon. J_s was higher in the morning than in the afternoon.

284 Diurnal time lag in the relation of J_s - R_s were influenced by VWC (Fig. 8, 9). For

285 example, J_s peaked about 2 h earlier than R_s on days with low VWC (Fig. 8a), 1 h earlier than
286 R_s on days with moderate VWC (Fig. 8b), and at the same time as R_s on days with high VWC
287 (Fig. 8c). Lag hours between J_s and R_s over the growing season were negatively and linearly
288 related to VWC (Fig. 9: Lag (h) = $-133.5 \times \text{VWC} + 12.24$, $R^2 = 0.41$). The effect of VWC on time
289 lags between J_s and R_s was smaller in 2014, with evenly distributed rainfall during the
290 growing season, than in 2013 with a pronounced summer drought (Fig. 9). Variables g_s and
291 Ω showed a significantly increasing trend with increasing VWC in 2013 and 2014 (Fig. 10).
292 This trend was more obvious in the dry year of 2013 than in 2014.

293

294 **4. Discussion and conclusions**

295 **4.1 Sap flow response to environmental factors**

296 Drought tolerance of some plants may be related to lower overall sensitivity of plant
297 physiological attributes to environmental stress and/or stomatal regulation (Huang et al.,
298 2011b; Naithani et al., 2012). In this study, larger regression slopes between J_s and the
299 environmental variables (R_s , VPD, and T) in the morning indicated that J_s was less sensitive
300 to variations in R_s , VPD, and T during the drier and hotter part of the day (Fig. 5). The
301 lower sensitivity combined with lower g_s led to lower J_s , and, thus, lower transpiration
302 (water consumption) during hot mid-day summer hours, pointing to a water-conservation
303 strategy in plant acclimation during dry and hot conditions. When R_s peaked during mid-
304 day (13:00-14:00 h) in summer, there was often insufficient soil water to meet the
305 atmospheric demand, causing g_s to be limited by available soil moisture and making J_s more
306 responsive to VWC at noon, but less responsive to R_s and T . Similarly, sap flow in
307 *Hedysarum mongolicum* and some other shrubs in a nearby region was positively correlated
308 with VWC at noon (Qian et al., 2015). For instance, sap flow in *Caragana korshinskii* was
309 significantly lower during the stress period, its conductance decreasing linearly after the
310 wilting point (She et al., 2013). The fact that J_s was less sensitive to meteorological
311 variables when $\text{VWC} < 0.10 \text{ m}^3 \text{ m}^{-3}$, highlights the water-conservation strategy taken by
312 drought-afflicted *Artemisia ordosica*. The positive linear relationship between g_s and VWC
313 in this study further supports this conclusion.

314 Precipitation, being the most important source of soil moisture and, thus, VWC, affected
315 transpiration directly. Frequent small rainfall events (< 5 mm) are crucially important to the
316 survival and growth of desert plants (Zhao and Liu, 2010). Variations in J_s were clearly
317 associated with the intermittent supply of water to the soil during rainfall events (see Fig. 2d,
318 f). Reduced J_s during rainy days can be largely explained by a reduction in incident R_s and
319 liquid water-induced saturation of the leaf surface, which led to a decrease in leaf turgor and
320 stomatal closure. After each rainfall event, J_s increased quickly when soil moisture was

321 replenished. Schwinning and Sala (2004) have previously shown that VWC contributed the
322 most to the post-rainfall response in plant transpiration at similar sites. The study shows that
323 *Artemisia ordosica* responded differently to wet and dry conditions. In the mid-growing
324 season, high J_s in July was related to rainfall-fed soil moisture, which increased the rate of
325 transpiration. However, dry soil conditions combined with high T and R_s led to a reduction
326 in J_s in August of 2013 (Fig. 2). In some deep-rooting desert shrubs, groundwater may
327 replenish water lost by transpiration (Yin et al., 2014). *Artemisia ordosica* roots are generally
328 distributed in the upper 60 cm of the soil (Zhao et al., 2010), and as a result the plant usually
329 depends on water directly supplied by precipitation because groundwater levels in drylands
330 can often be below the rooting zone of many shrub species, typically at depths ≥ 10 m as
331 witnessed at our site. Similar findings regarding the role of rainfall and VWC in desert
332 vegetation is reported by Wang et al. (2017).

333

334 **4.2 Hysteresis between sap flow and environmental factors**

335 Diurnal patterns in J_s corresponded with those of R_s from sunrise until diverging later in the
336 day (Fig. 7), suggesting that R_s was a primary controlling factor of diurnal J_s . As an initial
337 energy source, R_s also can force T and VPD to increase, causing a phase difference in time
338 lags among the relations of J_s - R_s , J_s - T , and J_s -VPD.

339 The hysteresis effect reflects plant acclimation to water limitations, due to g_s being
340 inherently dependent on plant hydrodynamics (Matheny et al. 2014). The large g_s in the
341 morning promoted higher rates of transpiration (Fig. 6, 7), while lower g_s in the afternoon
342 reduced transpiration. Therefore, diurnal curves (hysteresis) were mainly caused by a g_s -
343 induced hydraulic process (Fig. 7). The finding that hysteresis varied seasonally, decreasing
344 with increasing VWC, further reflects the acclimation to water limitation causing J_s to peak
345 in advance of the environmental factors. At our site, dry soils accompanied with high VPD
346 in summer, led to a decreased g_s and a more significant control of the stomata on J_s relative
347 to the environmental factors. The result that g_s increased with increasing VWC (Fig. 10a),
348 along with the synchronization of J_s and g_s , suggests that J_s is more sensitive to g_s in low
349 VWC and less so to R_s . Due to the incidence of small rainfall events in drylands, soil water
350 supplied by rainfall pulses was largely insufficient to meet the transpiration demand under
351 high mid-day R_s , resulting in clockwise loops. Lower Ω values (< 0.4) at our site also support
352 the idea that g_s have a greater control on transpiration than R_s under situations of water
353 limitation (Fig. 10).

354 Altogether, stomatal control on the diurnal evolution of J_s by reducing g_s combined with
355 lower sensitivity to meteorological variables during the mid-day dry hours help to reduce
356 water consumption in *Artemisia ordosica*. Seasonally, plant-moderated reductions in g_s and
357 increased hysteresis, leads to reduced J_s and acclimation to drought conditions. It is suggested

358 here that water limitation invokes a water-conservation strategy in *Artemisia ordosica*.
359 Contrary to our findings, counterclockwise hysteresis has been observed to occur between J_s
360 and R_s in tropical and temperate forests (Meinzer et al., 1997; O'Brien et al., 2004; Zeppel et
361 al., 2004), which is reported to be consistent with the capacitance of the particular soil-plant-
362 atmosphere system being considered. Unlike short-statured vegetation, it usually takes more
363 time for water to move up and expand vascular elements in tree stems during the transition
364 from night to day.

365

366 **4.3. Conclusions**

367 The relative influence of R_s , T , and VPD on J_s in *Artemisia ordosica* was modified by soil
368 water, indicating J_s 's lessened sensitivity to the environmental variables during dry periods.
369 J_s was constrained by soil water deficits, causing J_s to peak several hours prior to the peaking
370 of R_s . Diurnal hysteresis between J_s and R_s varied seasonally and was mainly controlled by
371 hydraulic stresses. Soil moisture controlled J_s response in *Artemisia ordosica* to
372 meteorological factors. This species acclimated to water limitations by invoking a water-
373 conservation strategy through stomatal regulation, producing a hysteresis effect. Our findings
374 add to our understanding of acclimation in desert-shrub species under stress of dehydration.

375 **Acknowledgments:** This research was financially supported by grants from the National
376 Natural Science Foundation of China (NSFC No. 31670710, 31670708, 31361130340),
377 the National Key Research and Development Program of China (2016YFC0500905), the
378 National Basic Research Program of China (Grant No. 2013CB429901), and the Academy
379 of Finland (Project No. 14921). Xin Jia and Wei Feng are also grateful to financial support
380 from the Fundamental Research Funds for the Central Universities (Proj. No. 2015ZCQ-SB-
381 02). This work is related to the Finnish-Chinese collaborative research project EXTREME
382 (2013-2016), between Beijing Forestry University (team led by Prof. Tianshan Zha) and the
383 University of Eastern Finland (team led by Prof. Heli Peltola), and the U.S. China Carbon
384 Consortium (USCCC). We thank Ben Wang, Sijing Li, Qiang Yang, and others for their
385 assistance in the field.

386

387 **References**

- 388 Asner, G. P., Archer, S., Hughes, R. F., Ansley, R. J., and Wessman, C. A.: Net changes in regional woody vegetation cover
389 and carbon storage in Texas Drylands, 1937–1999, *Global Change Biology*, 9, 316-335, 2003.
- 390 Baldocchi, D. D., Wilson, K. B., Gu, L.: How the environment, canopy structure and canopy physiological functioning
391 influence carbon, water and energy fluxes of a temperate broad-leaved deciduous forest – an assessment with the
392 biophysical model CANOAK, *Tree Physiology*, 22, 1065–1077, 2002.
- 393 Baldocchi, D. D.: The role of biodiversity on the evaporation of forests. In: Scherer-Lorenzen, M., Körner, C., Schulze, E.-
394 D. (Eds.), *Forest diversity and function ecological studies*, Springer, Berlin, Heidelberg, pp. 131–148, 2005.
- 395 Brouillette, L. C., Mason, C. M., Shirk, R. Y. and Donovan, L. A.: Adaptive differentiation of traits related to resource use

396 in a desert annual along a resource gradient, *New Phytologist*, 201: 1316–1327, 2014.

397 Buzkova, R., Acosta, M., Darenova, E., Pokorny, R., and Pavelka, M.: Environmental factors influencing the relationship
398 between stem CO₂ efflux and sap flow, *Trees-Struct Funct*, 29, 333-343, 2015.

399 Chen, Z. H., Zha, T., Jia, X., Wu, Y., Wu, B., Zhang, Y., Guo, J., Qin, S., Chen, S., and Peltola, H.: Leaf nitrogen is closely
400 coupled to phenophases in a desert shrub ecosystem in China, *Journal of Arid Environments*, 122, 124-131, 2015

401 Cochard, H., Barigah, S., Kleinhentz, M.: Is xylem cavitation resistance a relevant criterion for screening drought resistance
402 among *Prunus* species?, *Journal of Plant Physiology* 165: 976–982, 2008.

403 Cochard, H., Herbette, S., Hernandez, E.: The effects of sap ionic composition on xylem vulnerability to cavitation, *Journal*
404 *of Experimental Botany*, 61: 275–285, 2010.

405 Cowan, I.R., Farquhar, G.D.: Stomatal function in relation to leaf metabolism and environment, *Symposia of the Society*
406 *for Experimental Biology*, 31, 471–505, 1977.

407 Du, S., Wang, Y.-L., Kume, T., Zhang, J.-G., Otsuki, K., Yamanaka, N., and Liu, G.-B.: Sapflow characteristics and climatic
408 responses in three forest species in the semiarid Loess Plateau region of China, *Agricultural and Forest Meteorology*,
409 151, 1-10, 2011.

410 Dynamax: Dynagage® Installation and Operation Manual, Dynamax, Houston, TX, 2005.

411 Eberbach, P. L. and Burrows, G. E.: The transpiration response by four topographically distributed *Eucalyptus* species, to
412 rainfall occurring during drought in south eastern Australia, *Physiologia Plantarum*, 127, 483-493, 2006.

413 Ennajeh, M., Tounekti, T., Vadel, AM.: Water relations and droughtinduced embolism in olive (*Olea europaea*) varieties
414 ‘Meski’ and ‘Chemlali’ during severe drought, *Tree Physiology*, 28: 971–976, 2008..

415 Ewers, B.E., Mackay, D.S., Gower, S.T., Ahl, D.E., Samanta, S.N.B.: Tree species effects on stand transpiration in northern
416 Wisconsin, *Water Resources Research*, 38, 1– 11, 2002.

417 Ewers, B.E., Mackay, D.S., Samanta, S.: Interannual consistency in canopy stomatal conductance control of leaf water
418 potential across seven tree species, *Tree Physiology*, 27, 11–24, 2007.

419 Forner, A., Aranda, I., Granier, A., and Valladares, F.: Differential impact of the most extreme drought event over the last
420 half century on growth and sap flow in two coexisting Mediterranean trees, *Plant Ecol*, 215, 703-719, 2014.

421 Granier, A., Bréda, N., Biron, P., and Villette, S.: A lumped water balance model to evaluate duration and intensity of
422 drought constraints in forest stands, *Ecological Modelling*, 116(2), 269-283, 1999.

423 Granier, A., Reichstein, M., Bréda, N., Janssens, I. A., Falge, E., Ciais, P., and Buchmann, N.: Evidence for soil water
424 control on carbon and water dynamics in European forests during the extremely dry year, *Agricultural and forest*
425 *meteorology*, 143(1), 123-145, 2007.

426 Houghton, R. A., Hackler, J. L., and Lawrence, K. T.: The U.S. carbon budget: contributions from land-use change, *Science*,
427 285, 574-578, 1999.

428 Huang, H., Gang, W., and NianLai, C.: Advanced studies on adaptation of desert shrubs to environmental stress, *Sciences*
429 *in Cold and Arid Regions*, 3, 0455–0462, 2011a

430 Huang, L., Zhang, Z.S., and Li, X.R.: Sap flow of *Artemisia ordosica* and the influence of environmental factors in a
431 revegetated desert area: Tengger Desert, China, *Hydrological Processes*, 24, 1248-1253, 2010.

432 Huang, Y., Li, X., Zhang, Z., He, C., Zhao, P., You, Y., and Mo, L.: Seasonal changes in *Cyclobalanopsis glauca*
433 transpiration and canopy stomatal conductance and their dependence on subterranean water and climatic factors in
434 rocky karst terrain, *Journal of Hydrology*, 402, 135-143, 2011b.

435 Jacobsen, A. L., Agenbag, L., Esler, K. J., Pratt, R. B., Ewers, F. W., and Davis, S. D.: Xylem density, biomechanics and
436 anatomical traits correlate with water stress in 17 evergreen shrub species of the Mediterranean-type climate region of
437 South Africa, *Journal of Ecology*, 95, 171-183, 2007.

438 Jarvis, P. G.: The interpretation of the variations in leaf water potential and stomatal conductance found in canopies in the
439 field, *Philosophical Transactions of the Royal Society of London B: Biological Sciences*, 273, 593–610, 1976.

440 Jarvis, P. G., and McNaughton, K. G.: Stornatal Control of Transpiration: Scaling Up from Leaf’ to Region, *Advances in*

441 ecological research, 15, 1-42, 1986.

442 Jia, X., Zha, T., Wu, B., Zhang, Y., Gong, J., Qin, S., Chen, G., Kellomäki, S., and Peltola, H.: Biophysical controls on net
443 ecosystem CO₂ exchange over a semiarid shrubland in northwest China, *Biogeosciences* 11, 4679-4693, 2014.

444 Jia, X., Zha, T., Gong, J., Wang, B., Zhang, Y., Wu, B., Qin, S., and Peltola, H.: Carbon and water exchange over a temperate
445 semi-arid shrubland during three years of contrasting precipitation and soil moisture patterns, *Agricultural and Forest*
446 *Meteorology*, 228, 120-129, 2016.

447 Jian, S. Q., Wu, Z. N., Hu, C. H., and Zhang, X. L.: Sap flow in response to rainfall pulses for two shrub species in the
448 semiarid Chinese Loess Plateau, *J Hydrol Hydromech*, 64, 121-132, 2016.

449 Li, S. L., Weger, M. A., Zuidema, P., Yu, F., and Dong, M.: Seedlings of the semi-shrub *Artemisia ordosica* are resistant
450 to moderate wind denudation and sand burial in Mu Us sandland, China, *Trees*, 24, 515-521, 2010.

451 Li, S. J., Zha, T. S., Qin, S. G., Qian, D., and Jia, X.: Temporal patterns and environmental controls of sap flow in *Artemisia*
452 *ordosica*, *Chinese Journal of Ecology*, 33, 1-7, 2014.

453 Lioubimtseva, E. and Henebry, G. M.: Climate and environmental change in arid Central Asia: Impacts, vulnerability, and
454 adaptations, *Journal of Arid Environments*, 73, 963-977, 2009.

455 Liu, B., Zhao, W., and Jin, B.: The response of sap flow in desert shrubs to environmental variables in an arid region of
456 China, *Ecohydrology*, 4, 448-457, 2011.

457 Matheny, A. M., Bohrer, G., Vogel, C. S., Morin, T. H., He, L., Frasson, R. P. D. M., Mirfenderesgi, G., Schäfer, K. V. R.,
458 Gough, C. M., Ivanov, V. Y., and Curtis, P. S.: Species - specific transpiration responses to intermediate disturbance
459 in a northern hardwood forest, *Journal of Geophysical Research: Biogeosciences*, 119(12), 2292-2311, 2014.

460 McAdam, S. A., Sussmilch, F. C. and Brodribb, T. J.: Stomatal responses to vapour pressure deficit are regulated by high
461 speed gene expression in angiosperms, *Plant, Cell and Environment*, 39, 485-491, 2016.

462 McDowell, N. G., Fisher, R. A., Xu, C.: Evaluating theories of drought-induced vegetation mortality using a multimodel-
463 experiment framework, *New Phytologist*, 200 (2), 304-321, 2013.

464 Meinzer, F. C., Andrade, J. L., Goldstein, G., Holbrook, N. M., Cavellier, J., and Jackson, P.: Control of transpiration from
465 the upper canopy of a tropical forest: the role of stomatal, boundary layer and hydraulic architecture components, *Plant,*
466 *Cell and Environment*, 20, 1242-1252, 1997.

467 Naithani, K. J., Ewers, B. E., and Pendall, E.: Sap flux-scaled transpiration and stomatal conductance response to soil and
468 atmospheric drought in a semi-arid sagebrush ecosystem, *Journal of Hydrology*, 464, 176-185, 2012.

469 O'Brien, J. J., Oberbauer, S. F., and Clark, D. B.: Whole tree xylem sap flow responses to multiple environmental variables
470 in a wet tropical forest, *Plant, Cell & Environment*, 27, 551-567, 2004.

471 Pacala, S. W., Hurtt, G. C., Baker, D., Peylin, P., Houghton, R. A., Birdsey, R. A., Heath, L., Sundquist, E. T., Stallard, R.
472 F., Ciais, P., Moorcroft, P., Caspersen, J. P., Shevliakova, E., Moore, B., Kohlmaier, G., Holland, E., Gloor, M.,
473 Harmon, M. E., Fan, S.-M., Sarmiento, J. L., Goodale, C. L., Schimel, D., and Field, C. B.: Consistent land- and
474 atmosphere-based U.S. carbon sink estimates, *Science*, 292, 2316-2320, 2001.

475 Qian, D., Zha, T., Jia, X., Wu, B., Zhang, Y., Bourque, C. P., Qin, S., and Peltola, H.: Adaptive, water-conserving strategies
476 in *Hedysarum mongolicum* endemic to a desert shrubland ecosystem, *Environmental Earth Sciences*, 74(7), 6039, 2015.

477 Razzaghi, F., Ahmadi, S. H., Adolf, V. I., Jensen, C. R., Jacobsen, S. E., and Andersen, M. N.: Water relations and
478 transpiration of quinoa (*Chenopodium quinoa* Willd.) under salinity and soil drying, *Journal of Agronomy and Crop*
479 *Science*, 197, 348-360, 2011.

480 Schwinning, S. and Sala, O. E.: Hierarchy of responses to resource pulses in arid and semi-arid ecosystems, *Oecologia*, 141,
481 211-220, 2004.

482 She, D., Xia, Y., Shao, M., Peng, S., and Yu, S.: Transpiration and canopy conductance of *Caragana korshinskii* trees in
483 response to soil moisture in sand land of China, *Agroforestry systems*, 87, 667-678, 2013.

484 Sus, O., Poyatos, R., Barba, J., Carvalhais, N., Llorens, P., Williams, M., and Vilalta, J. M.: Time variable hydraulic
485 parameters improve the performance of a mechanistic stand transpiration model. A case study of Mediterranean Scots

486 pine sap flow data assimilation, *Agricultural and Forest Meteorology*, 198–199, 168–180, 2014.

487 Wang, X. P., Schaffer, B. E., Yang, Z. and Rodriguez-Iturbe, I.: Probabilistic model predicts dynamics of vegetation biomass
488 in a desert ecosystem in NW China. *Proceedings of the National Academy of Sciences*, 201703684, 2017.

489 Yin, L., Zhou, Y., Huang, J., Wenninger, J., Hou, G., Zhang, E., Wang, X., Dong, J., Zhang, J., and Uhlenbrook, S.:
490 Dynamics of willow tree (*Salix matsudana*) water use and its response to environmental factors in the semi-arid Hailiutu
491 River catchment, Northwest China, *Environmental earth sciences*, 71, 4997-5006, 2014.

492 Zeppel, M. J. B., Murray, B. R., Barton, C., and Eamus, D.: Seasonal responses of xylem sap velocity to VPD and solar
493 radiation during drought in a stand of native trees in temperate Australia, *Functional Plant Biology*, 31, 461-470, 2004.

494 Zeppel, M.: Convergence of tree water use and hydraulic architecture in water - limited regions: a review and synthesis,
495 *Ecohydrology*, 6(5), 889-900, 2013.

496 Zha, T., Li, C., Kellomäki, S., Peltola, H., Wang, K.-Y., and Zhang, Y.: Controls of evapotranspiration and CO² fluxes from
497 scots pine by surface conductance and abiotic factors, *PloS one*, 8, e69027, 2013.

498 Zhao, W. and Liu, B.: The response of sap flow in shrubs to rainfall pulses in the desert region of China, *Agricultural and*
499 *Forest Meteorology*, 150, 1297-1306, 2010.

500 Zhao, Y., Yuan, W., Sun, B., Yang, Y., Li, J., Li, J., Cao, B., and Zhong, H.: Root distribution of three desert shrubs and
501 soil moisture in Mu Us sand land, *Research of Soil and Water Conservation*, 17, 129-133, 2010.

502 Zheng, C. and Wang, Q.: Water-use response to climate factors at whole tree and branch scale for a dominant desert species
503 in central Asia: *Haloxylon ammodendron*, *Ecohydrology*, 7, 56-63, 2014.

504

505

506 **Table 1** Seasonal changes in monthly transpiration (T_r), leaf area index (LAI), and stomatal
 507 conductance (g_s) in *Artemisia ordosica* during the growing seasons (May-September period)
 508 of 2013 and 2014.

	T_r (mm mon ⁻¹)		LAI (m ² m ⁻²)		g_s (mol m ⁻² s ⁻¹)	
	2013	2014	2013	2014	2013	2014
May	0.57	1.59	0.02	0.04	0.07	0.18
June	1.03	2.28	0.05	0.06	0.08	0.13
July	3.36	3.46	0.10	0.06	0.09	0.14
August	1.04	2.45	0.08	0.06	0.10	0.08
September	1.23	1.13	0.05	0.04	0.15	0.05

509

510

511

512 **Table 2** Mean monthly diurnal cycles of sap flow (J_s) response to shortwave radiation (R_s),
 513 air temperature (T), and water vapor pressure deficit (VPD), including time lags (h) as a
 514 function of R_s , T , and VPD.

515

Relationship	May		June		July		August		September	
	2013	2014	2013	2014	2013	2014	2013	2014	2013	2014
J_s-R_s	5	2	3	0	2	1	3	1	3	2
J_s-T	8	6	7	4	4	4	6	5	6	6
J_s-VPD	8	5	7	4	6	4	6	5	6	5

516

517

518

519 **Figure captions:**

520 **Fig. 1** Sap flow per leaf area (J_s) as a function of soil water content (VWC) at 30-cm depth
521 in non-rainy, daytime hours during the mid-growing period from June 1-August 31, 2013 and
522 2014. Data points are binned values from pooled data over two years at a VWC increment of
523 $0.003 \text{ m}^3 \text{ m}^{-3}$. Dotted line represents the VWC threshold for J_s .

524

525 **Fig. 2** Seasonal changes in daily (24-hour) mean shortwave radiation (R_s ; a), air temperature
526 (T ; b), water vapor pressure deficit (VPD; c), volumetric soil water content (VWC; d),
527 relative extractable water (REW; e), daily total precipitation (PPT; d), and daily sap flow per
528 leaf area (J_s ; f), and daily transpiration (T_r , mm d^{-1} ; f) from May to September for both 2013
529 and 2014. Horizontal dash lines (d, e) represent VWC and REW threshold of $0.1 \text{ m}^3 \text{ m}^{-3}$ and
530 0.4 , respectively. Shaded bands indicate periods of drought.

531

532 **Fig. 3** Relationships between sap flow per leaf area (J_s) and environmental factors [shortwave
533 radiation (R_s), air temperature (T), water vapor pressure deficit (VPD), and soil water content
534 at 30-cm depth (VWC)] in non-rainy days between 8:00-20:00 h during the mid-growing
535 season of June 1-August 31 for 2013 and 2014. Data points are binned values from pooled
536 data over two years at increments of 40 W m^{-2} , 1.2°C , 0.3 kPa , and $0.005 \text{ m}^3 \text{ m}^{-3}$ for R_s , T ,
537 VPD and VWC, respectively.

538

539 **Fig. 4** Sap flow per leaf area (J_s) in non-rainy, daytime hours during the mid-growing season
540 of June 1-August 31 for both 2013 and 2014 as a function of shortwave radiation (R_s), air
541 temperature (T), water vapor pressure deficit (VPD) under high volumetric soil water content
542 ($\text{VWC} > 0.10 \text{ m}^3 \text{ m}^{-3}$ both in 2013 and 2014) and low VWC ($< 0.10 \text{ m}^3 \text{ m}^{-3}$, 2013 and 2014).
543 J_s is given as binned averages according to R_s , T , and VPD, based on increments of 100 W
544 m^{-2} , 1°C , and 0.2 kPa , respectively. Bars indicate standard error.

545

546 **Fig. 5** Regression slopes of linear fits between sap flow per leaf area (J_s) in non-rainy days
547 and shortwave radiation (R_s), water vapor pressure deficit (VPD), air temperature (T), and
548 volumetric soil water content (VWC) between 8:00-20:00 h during the mid-growing season
549 of June 1-August 31 for 2013 and 2014.

550

551 **Fig. 6** Mean monthly diurnal changes in sap flow per leaf area (J_s) and stomatal conductance
552 (g_s) in *Artemisia ordosica* during the growing season (May-September period) for both 2013
553 and 2014. Each point is given as the mean at specific times during each month.

554

555 **Fig. 7** Seasonal variation in hysteresis between sap flow per leaf area (J_s) and shortwave

556 radiation (R_s) using normalized plots for both 2013 and 2014. The y-axis represents the
557 proportion of maximum J_s (dimensionless), and the x-axis represents the proportion of
558 maximum R_s (dimensionless). The curved arrows indicate the clockwise direction of response
559 during the day.

560

561 **Fig. 8** Sap flow per leaf area (J_s) and shortwave radiation (R_s) over consecutive three days in
562 2013, i.e., (a) under low volumetric soil water content (VWC) and high water vapor pressure
563 deficit (VPD; DOY 153-155, VWC=0.064 m³ m⁻³, REW=0.025, VPD=2.11 kPa), (b)
564 moderate VWC and VPD (DOY 212-214, VWC=0.092 m³ m⁻³, REW=0.292, VPD=1.72
565 kPa), and (c) high VWC and low VPD (DOY 192-194, VWC=0.152 m³ m⁻³, REW=0.865,
566 VPD= 0.46 kPa); REW is the relative extractable soil water. VWC, REW, and VPD are the
567 3-day mean value.

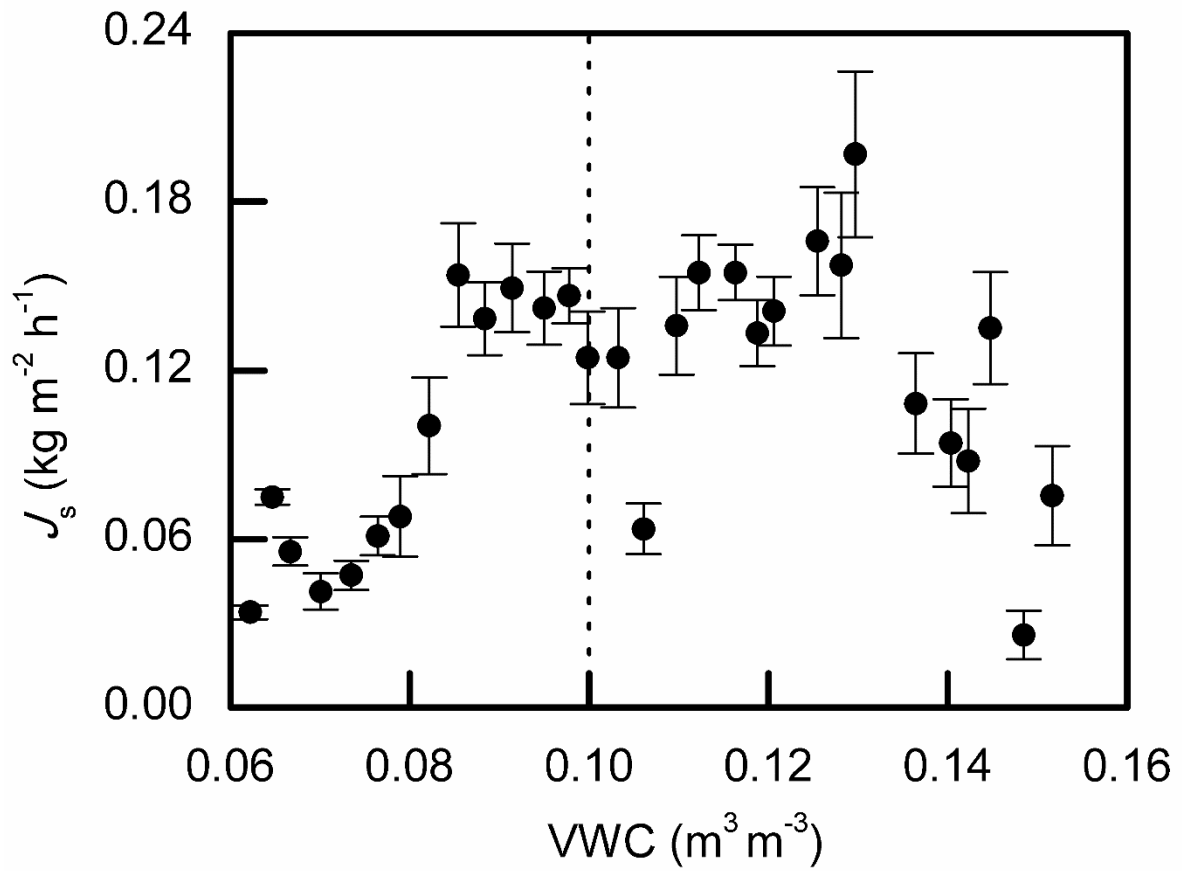
568

569 **Fig. 9** Time lag between sap flow per leaf area (J_s) and short wave radiation (R_s) in relation
570 to volumetric soil water content (VWC). Hourly data in non-rainy days during the mid-
571 growing season of June 1-August 31 for 2013 and 2014. The lag hours were calculated by a
572 cross-correlation analysis using a three-day moving window with a one-day time step. Rainy
573 days were excluded. The solid line is based on exponential regression ($p<0.05$).

574

575 **Fig. 10** Relationship between volumetric soil water content (VWC) and (a) stomatal
576 conductance (g_s) in *Artemisia ordosica*, and (b) decoupling coefficient (Ω) for 2013 and 2014.
577 Hourly values are given as binned averages based on a VWC-increment of 0.005 m³ m⁻³.
578 Bars indicate standard error. Only statistically significant regressions (with p -values < 0.05)
579 are shown.

580



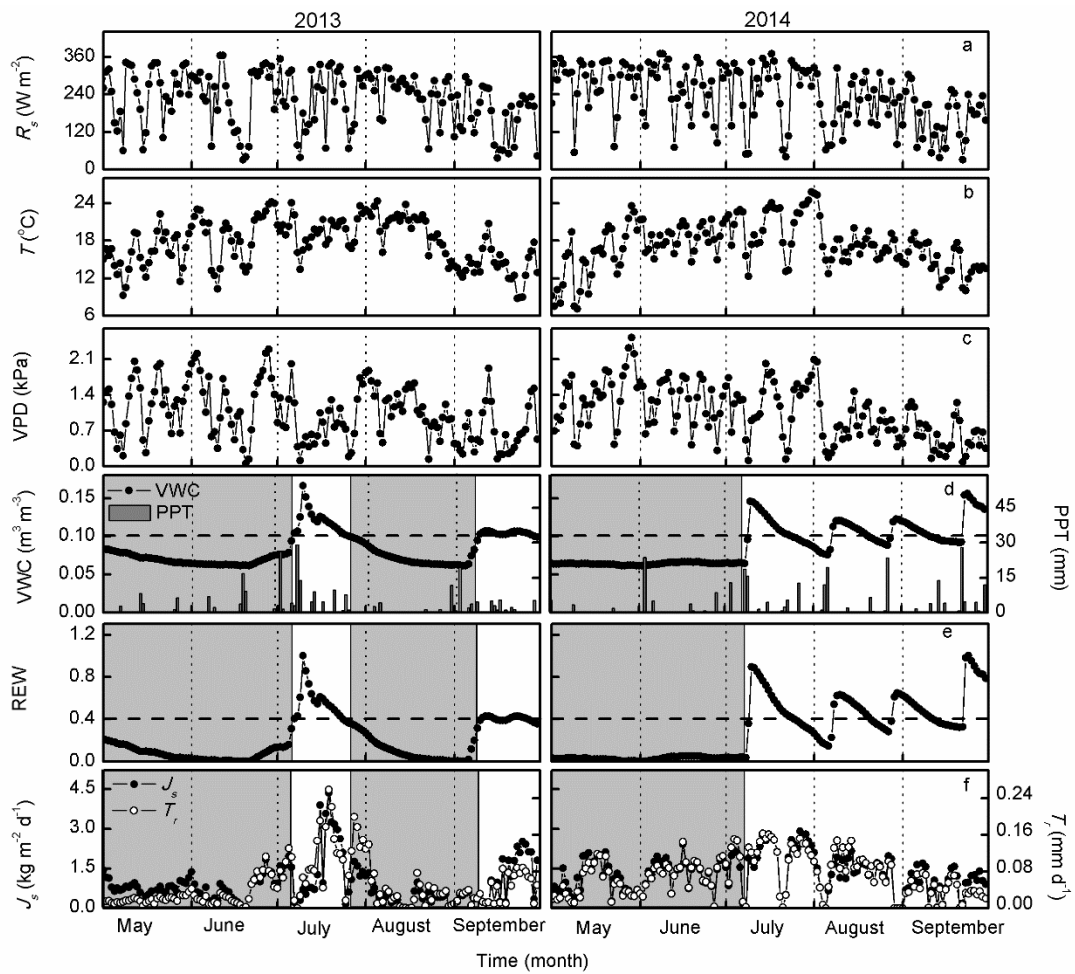
582

583 **Fig. 1** Sap flow per leaf area (J_s) as a function of soil water content (VWC) at 30-cm depth
 584 in non-rainy, daytime hours during the mid-growing period from June 1-August 31, 2013 and
 585 2014. Data points are binned values from pooled data over two years at a VWC increment of
 586 $0.003 \text{ m}^3 \text{ m}^{-3}$. Dotted line represents the VWC threshold for J_s .

587

588

589



591

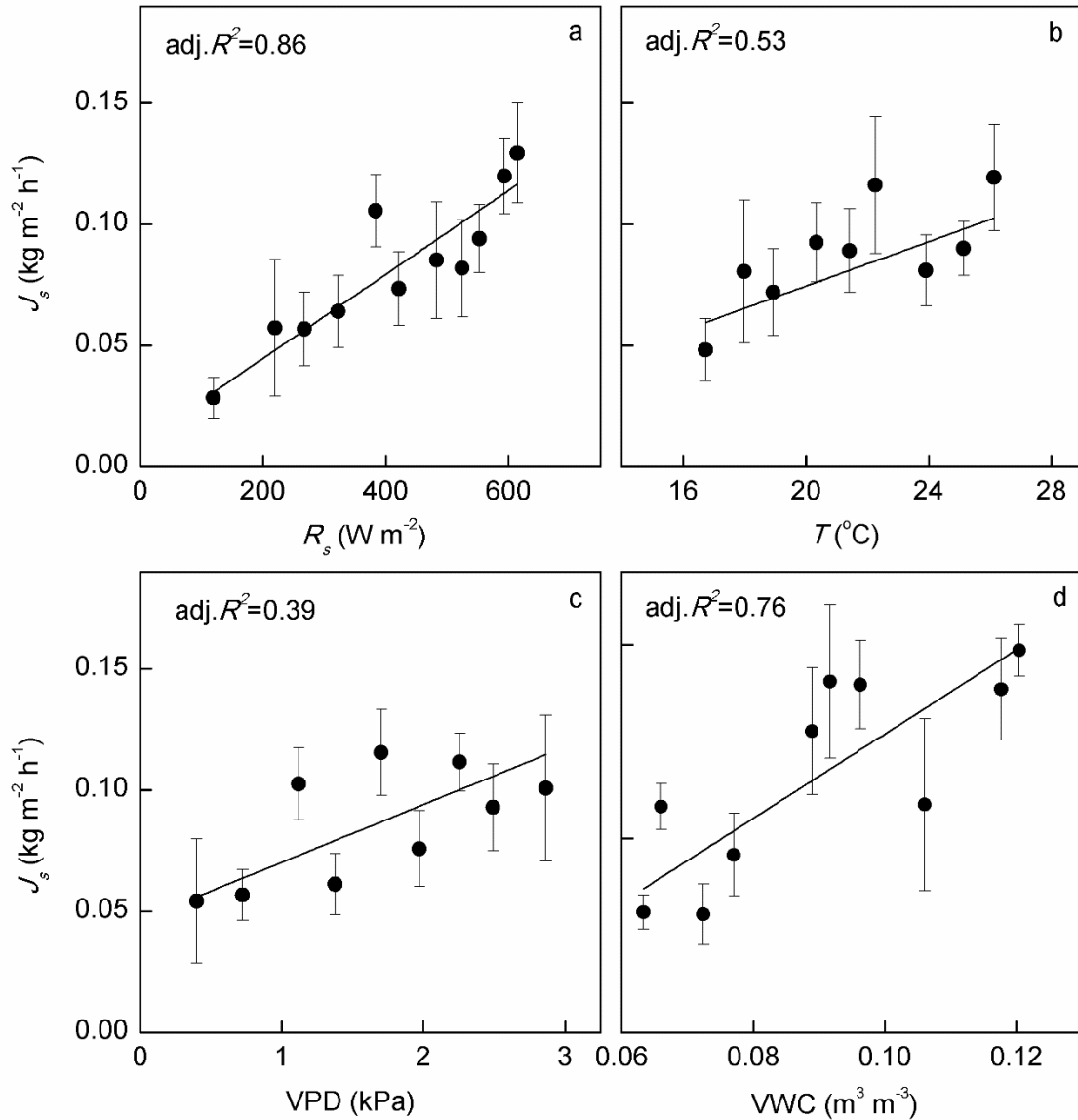
592

593 **Fig. 2** Seasonal changes in daily (24-hour) mean shortwave radiation (R_s ; a), air temperature
 594 (T ; b), water vapor pressure deficit (VPD; c), volumetric soil water content (VWC; d),
 595 relative extractable water (REW; e), daily total precipitation (PPT; d), and daily sap flow per
 596 leaf area (J_s ; f), and daily transpiration (T_r , mm d^{-1} ; f) from May to September for both 2013
 597 and 2014. Horizontal dash lines (d, e) represent VWC and REW threshold of $0.1 \text{ m}^3 \text{ m}^{-3}$ and
 598 0.4 , respectively. Shaded bands indicate periods of drought.

599

600

601



602

603

604

605

606

607

608

609

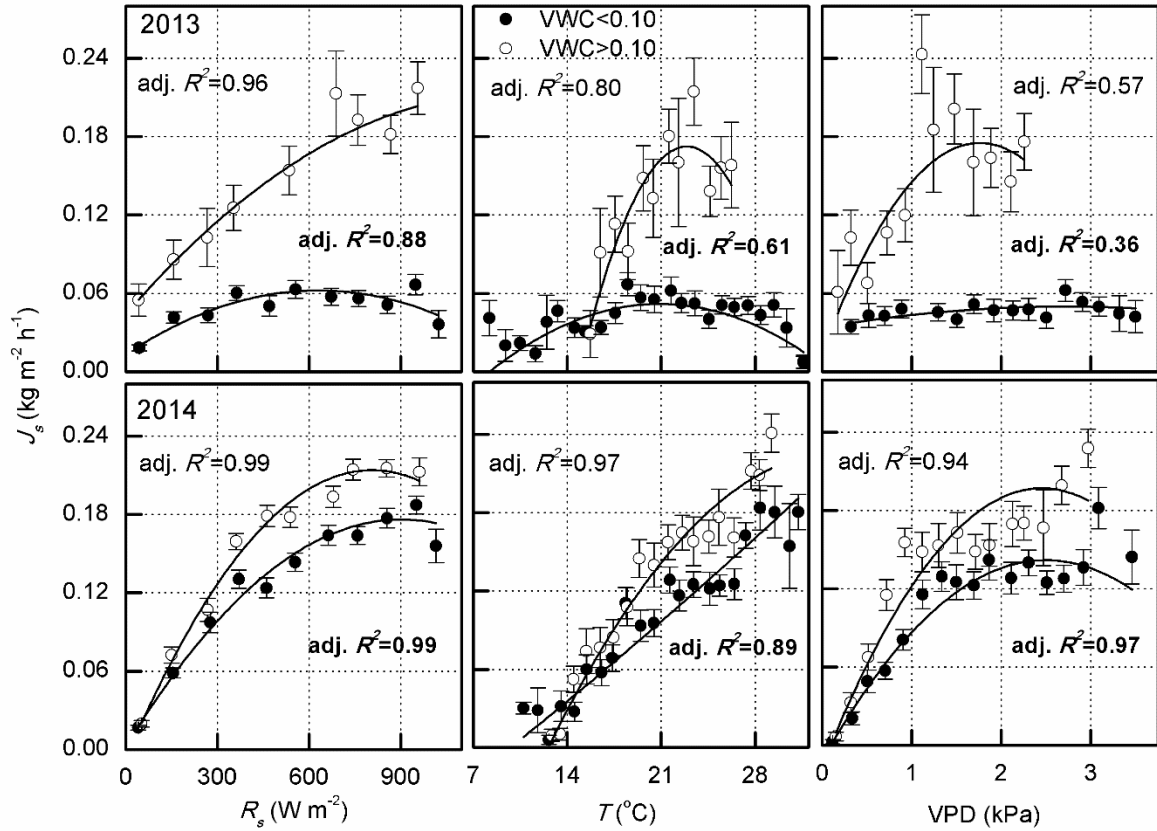
610

611

612

613

Fig. 3 Relationships between sap flow per leaf area (J_s) and environmental factors [shortwave radiation (R_s), air temperature (T), water vapor pressure deficit (VPD), and soil water content at 30-cm depth (VWC)] in non-rainy days between 8:00-20:00 h during the mid-growing season of June 1-August 31 for 2013 and 2014. Data points are binned values from pooled data over two years at increments of 40 W m^{-2} , 1.2°C , 0.3 kPa , and $0.005 \text{ m}^3 \text{ m}^{-3}$ for R_s , T , VPD and VWC, respectively.



614

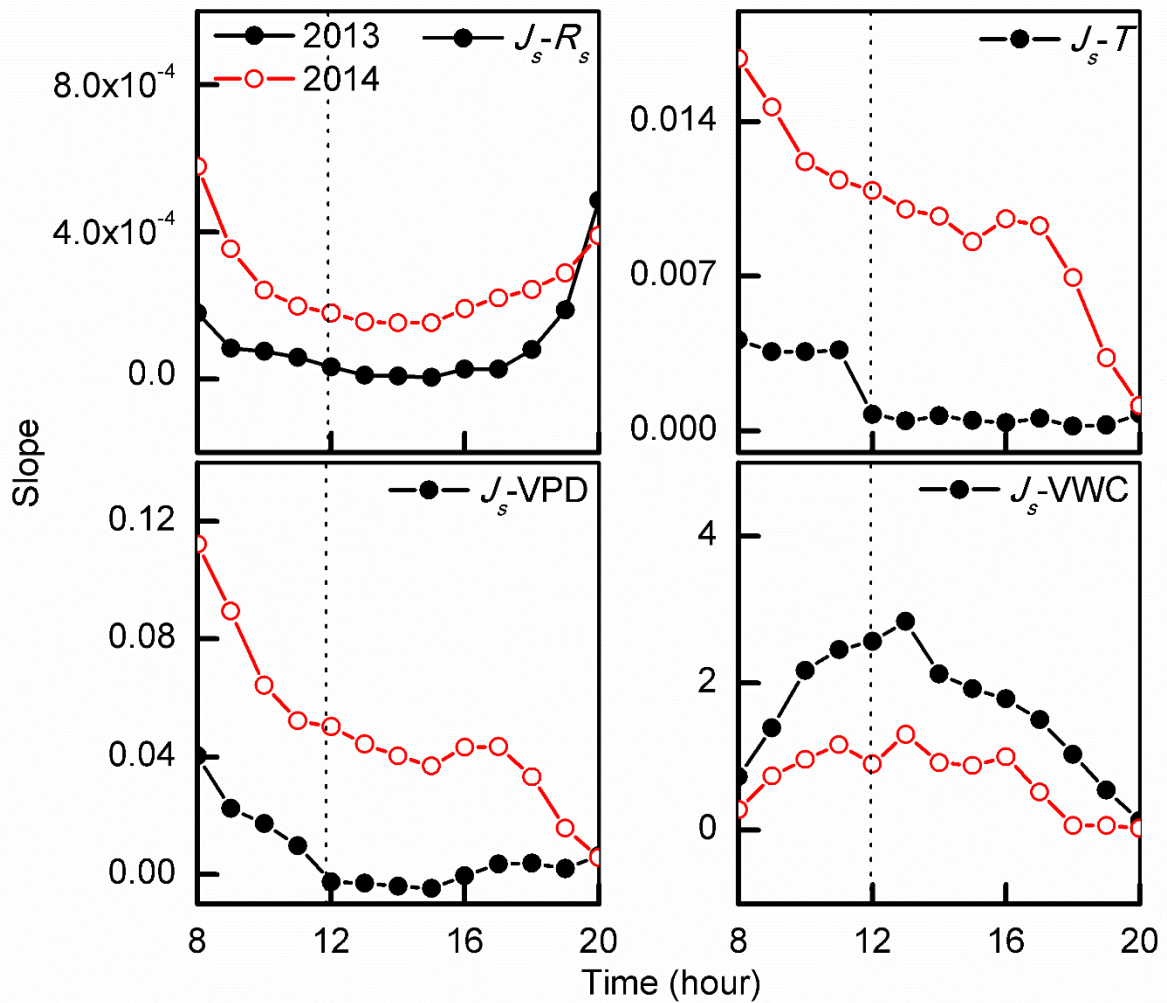
615

616 **Fig. 4** Sap flow per leaf area (J_s) in non-rainy, daytime hours during the mid-growing season
 617 of June 1-August 31 for both 2013 and 2014 as a function of shortwave radiation (R_s), air
 618 temperature (T), water vapor pressure deficit (VPD) under high volumetric soil water content
 619 ($VWC > 0.10 m^3 m^{-3}$ both in 2013 and 2014) and low $VWC (< 0.10 m^3 m^{-3}$, 2013 and 2014).
 620 J_s is given as binned averages according to R_s , T , and VPD, based on increments of $100 W$
 621 m^{-2} , $1^{\circ}C$, and $0.2 kPa$, respectively. Bars indicate standard error.

622

623

624

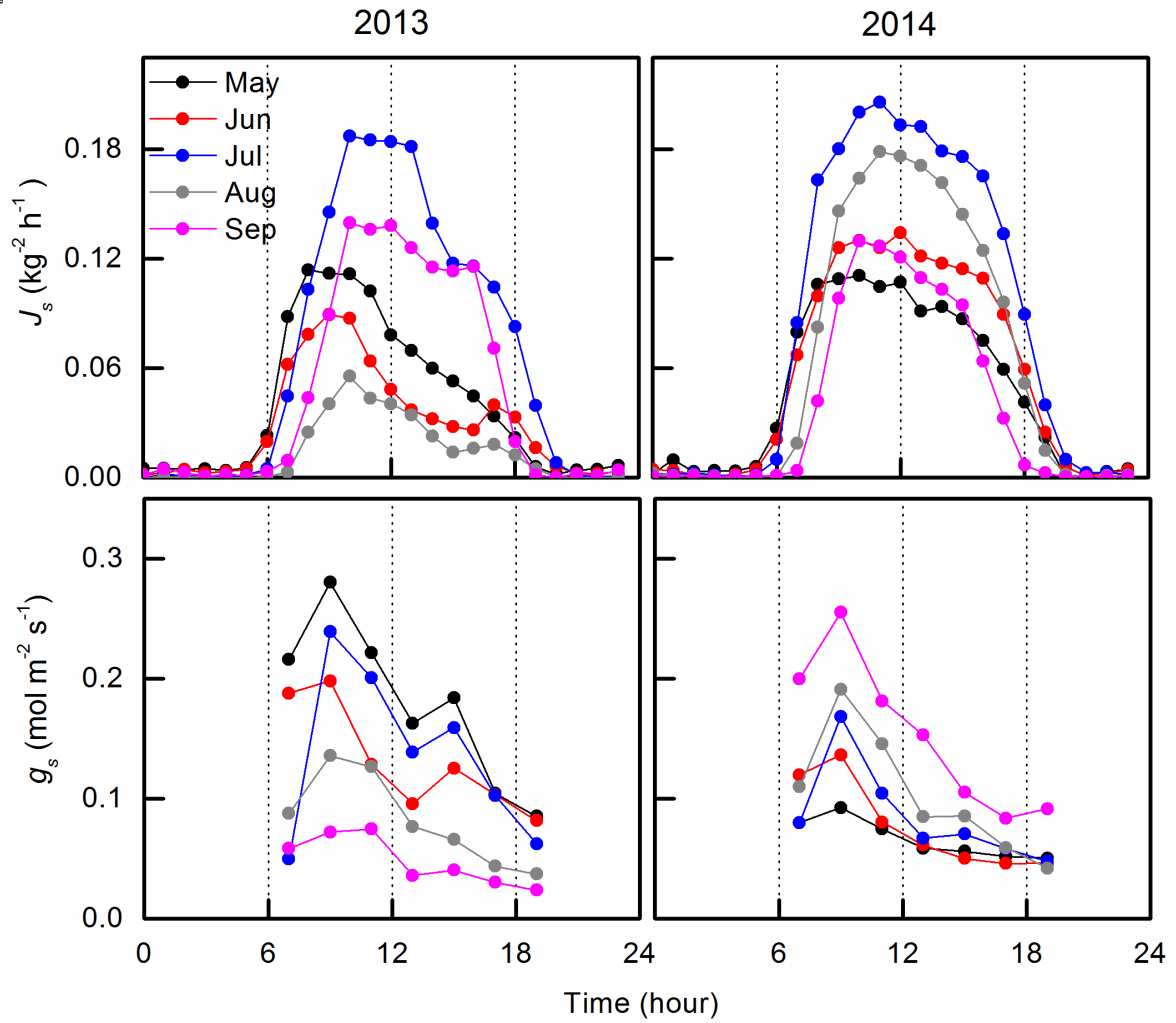


626

627 **Fig. 5** Regression slopes of linear fits between sap flow per leaf area (J_s) in non-rainy days
 628 and shortwave radiation (R_s), water vapor pressure deficit (VPD), air temperature (T), and
 629 volumetric soil water content (VWC) between 8:00-20:00 h during the mid-growing season
 630 of June 1-August 31 for 2013 and 2014.

631

632



634

635

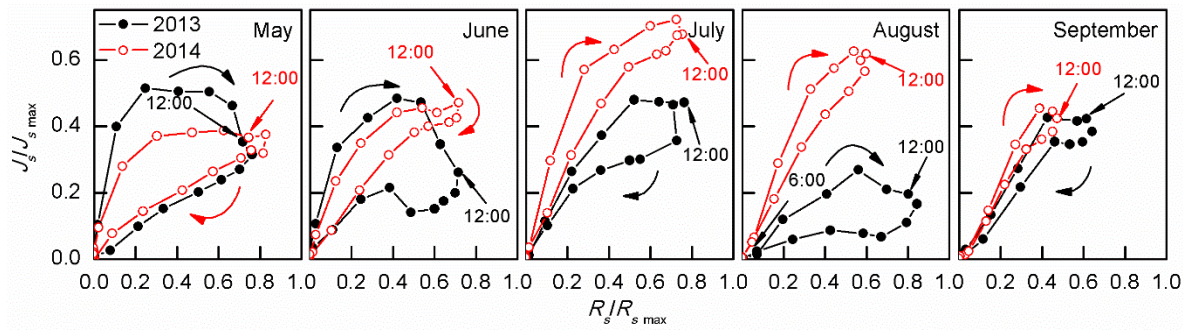
636 **Fig. 6** Mean monthly diurnal changes in sap flow per leaf area (J_s) and stomatal conductance
 637 (g_s) in *Artemisia ordosica* during the growing season (May-September period) for both 2013
 638 and 2014. Each point is given as the mean at specific times during each month.

639

640

641

642



643

644

645 **Fig. 7** Seasonal variation in hysteresis between sap flow per leaf area (J_s) and shortwave
646 radiation (R_s) using normalized plots for both 2013 and 2014. The y-axis represents the
647 proportion of maximum J_s (dimensionless), and the x-axis represents the proportion of
648 maximum R_s (dimensionless). The curved arrows indicate the clockwise direction of response
649 during the day.

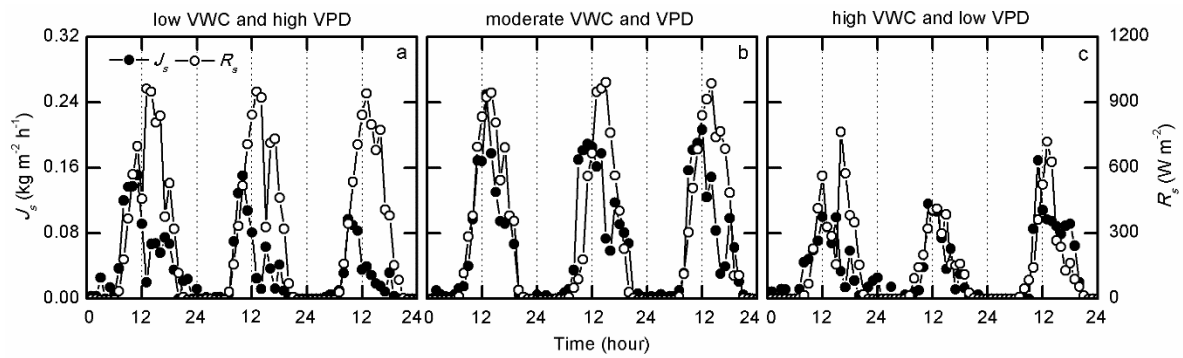
650

651

652

653

654

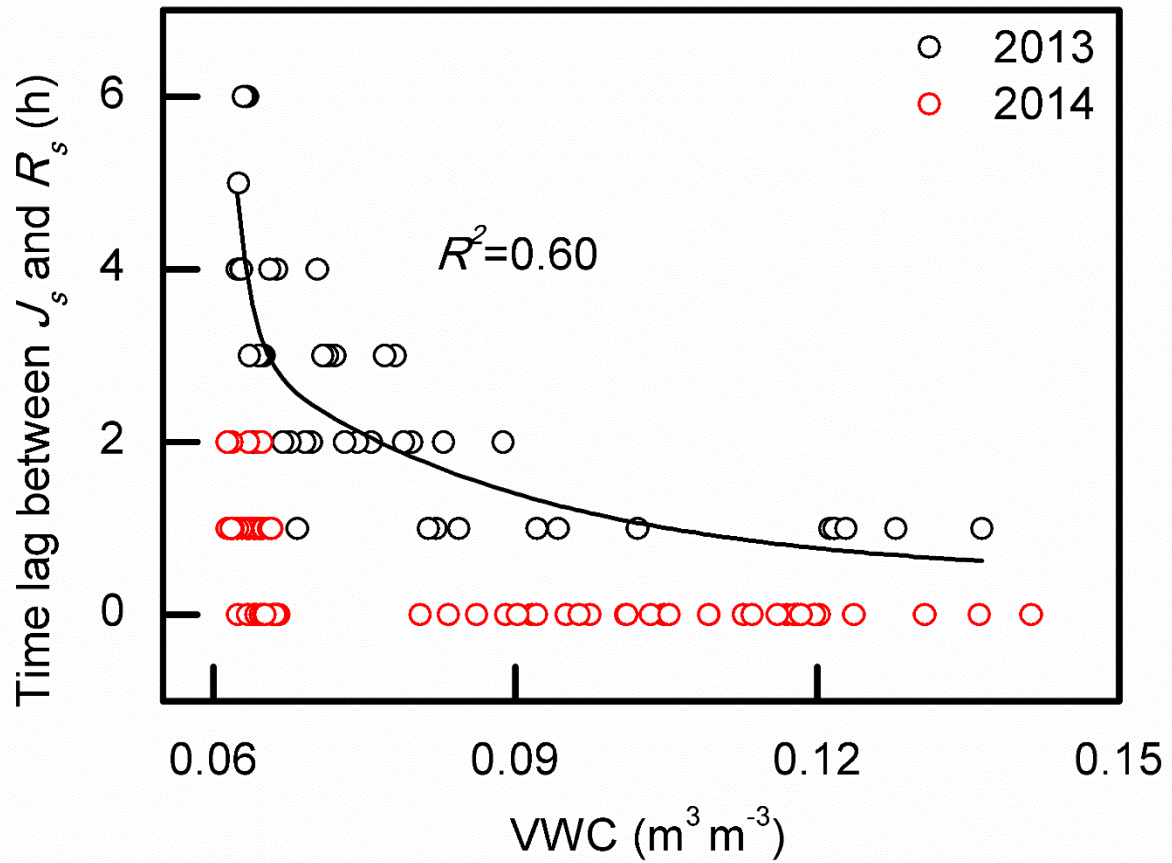


655

656

657 **Fig. 8** Sap flow per leaf area (J_s) and shortwave radiation (R_s) over consecutive three days in
658 2013, i.e., (a) under low volumetric soil water content (VWC) and high water vapor pressure
659 deficit (VPD; DOY 153-155, VWC=0.064 m³ m⁻³, REW=0.025, VPD=2.11 kPa), (b)
660 moderate VWC and VPD (DOY 212-214, VWC=0.092 m³ m⁻³, REW=0.292, VPD=1.72
661 kPa), and (c) high VWC and low VPD (DOY 192-194, VWC=0.152 m³ m⁻³, REW=0.865,
662 VPD= 0.46 kPa); REW is the relative extractable soil water. VWC, REW, and VPD are the
663 3-day mean value.

664



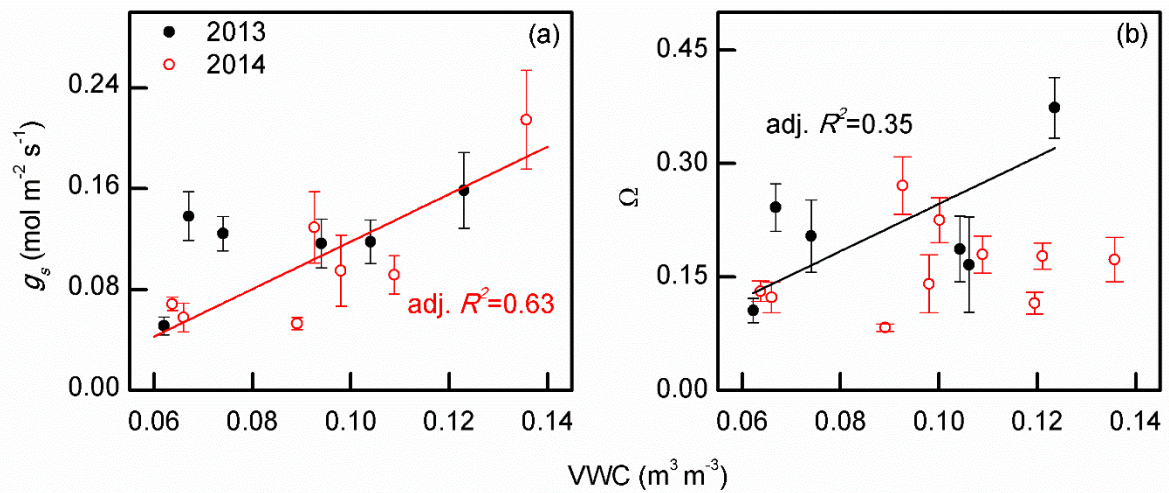
665

666

667 **Fig. 9** Time lag between sap flow per leaf area (J_s) and short wave radiation (R_s) in relation
 668 to volumetric soil water content (VWC). Hourly data in non-rainy days during the mid-
 669 growing season of June 1-August 31 for 2013 and 2014. The lag hours were calculated by a
 670 cross-correlation analysis using a three-day moving window with a one-day time step. Rainy
 671 days were excluded. The solid line is based on exponential regression ($p < 0.05$).

672

673



675

676

677 **Fig. 10** Relationship between volumetric soil water content (VWC) and (a) stomatal
 678 conductance (g_s) in *Artemisia ordosica*, and (b) decoupling coefficient (Ω) for 2013 and 2014.
 679 Hourly values are given as binned averages based on a VWC-increment of 0.005 m³ m⁻³.
 680 Bars indicate standard error. Only statistically significant regressions (with p -values < 0.05)
 681 are shown.

682